

PRINTED CIRCUIT BOARD WINDINGS-BASED ULTRA LOW-PROFILE POWER CONDITIONING CIRCUITS FOR SDR APPLICATION SYSTEMS

Wonseok Lim (Kyungpook National University, Taegu, Korea; iws95@ee.knu.ac.kr);
Dongsoo Kim (Kyungpook National University, Taegu, Korea; kds222s@hanmail.net); and
Byungcho Choi (Kyungpook National University, Taegu, Korea; bchoi@ee.kyungpook.ac.kr)

ABSTRACT

This paper presents two new power conversion circuits developed for future SDR application systems. The first power conditioning circuit is a contactless battery charger that employs a pair of separate printed circuit board (PCB) windings as a contactless energy transfer device. The second circuit is an ultra low-profile dc-to-dc converter that utilizes a pair of PCB windings (printed on opposite sides of a double-sided PCB) as a coreless transformer. By using PCB windings an energy transfer device, the proposed power conditioning circuits readily implement a low-profile design, which is critically needed for SDR application systems.

1. INTRODUCTION

Earlier studies [1, 2] have shown that a substantial inductive coupling exists between two neighboring copper windings printed on the surface of printed circuit boards (PCBs). When a pair of separate PCB windings are placed closely in parallel, the inductive coupling between PCB windings can be used as a means of contactless energy transfer [3]. On the other hand, when a pair of copper windings are printed on opposite sides of a double-sided PCB, the double-sided PCB can be used as a substitute for a conventional core-based transformer [4]. The use of PCB windings as an energy transfer device allows the corresponding power conditioning circuit to be fabricated in an ultra low-profile fashion. Accordingly, the resulting power conditioning circuit can be readily applied to future SDR application systems, which impose stringent requirements on height, space, and reliability of their power supplies. This paper presents a contactless battery charger and ultra low-profile dc-to-dc converter developed for such applications.

This work was supported in part by HY-SDR Research Center at Hanyang University, Seoul, Korea, under the ITRC program of MIC, Korea, and in part by the Regional Research Center Program of the Ministry of Commerce, Industry, and Energy of Korea.

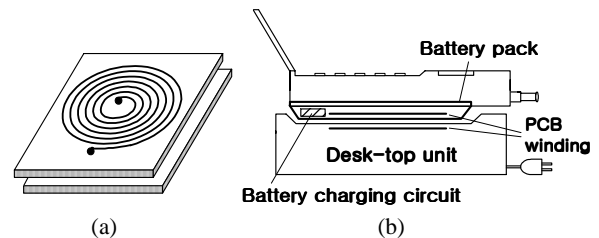


Fig. 1. Neighboring PCB windings and contactless charger for cellular phones. (a) Neighboring PCB windings. (b) Contactless charger developed for cellular phones.

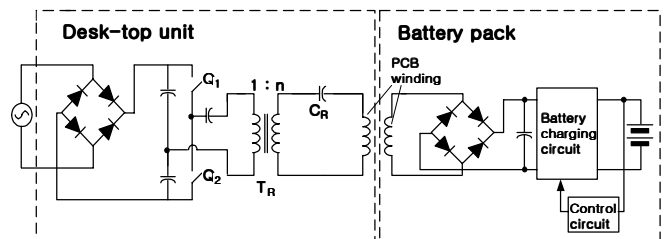


Fig. 2. Simplified circuit diagram of proposed contactless charger.

2. CONTACTLESS BATTERY CHARGER

2.1. Structure and Circuit Topology

When a pair of separate PCB windings (each built on a single-sided PCB) are closely placed in parallel (Fig. 1(a)), the inductive coupling between PCB windings can be used as a means of contactless energy transfer [3]. Fig. 1(b) shows the structure of the proposed contactless charger, developed for cellular phones based on the aforementioned contactless energy transfer concept. The desk-top unit (the primary side of the charger) contains the primary PCB winding together with associate electronics. The secondary side of the charger, containing the secondary PCB winding and battery charging/controlling circuit, is fabricated inside a standard battery pack, as shown in Fig. 1(b).

TABLE I: OPERATIONAL CONDITIONS AND CIRCUIT PARAMETERS OF PROTOTYPE CHARGER.

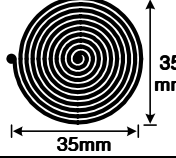
Desk-top unit	Secondary side
Input voltage: $85 \sim 270 V_{ac}$ Switching frequency: $f_S = 950 \text{ kHz}$	Input voltage of battery charging circuit: $8 \sim 20 V_{dc}$ Input current of battery charging circuit: $0.1 \sim 0.35 A_{dc}$
Circuit components: $Q_1 \sim Q_2$: IRF840 C_R : 40 nF $n = 0.1$	Control IC: LT1571-5 Battery: Type: 3.3W Li-ion Dimension: $55\text{mm} \times 31\text{mm} \times 5.5\text{mm}$ Voltage: $3.6 \sim 4.2 V$ Charging current: $0.8 A$ @ fast charging

Fig. 2 shows a simplified circuit diagram of the proposed contactless battery charger. The desk-top unit consists of a line-frequency rectifier, high-frequency inverter, and primary PCB winding. A half-bridge series resonant circuit is selected for the inverter topology as it utilizes the leakage inductance of the PCB windings as an element of the resonant tank circuit. The use of a resonant circuit is also advantages as it minimizes the harmonic components in the circuit waveforms, thereby easing the electromagnetic interference (EMI) problem that can be incurred by the PCB windings in operation. In addition, a half-bridge series resonant circuit readily achieves a high frequency operation, which is essential to reduce the circulating current. A conventional step-down transformer T_R is inserted between the half-bridge switch network and the resonant tank to further reduce the circulating current.

The secondary side of the charger consists of the secondary PCB winding, high-frequency rectifier, and battery charging circuit. The battery charging/controlling circuit is designed using the LT1571-5 [5] that contains the power switches, pulse-width modulation block, feedback control circuit, and other circuits needed to monitor and control the battery charging current. For this particular application, the charging circuit can be miniaturized without causing major thermal management problems and therefore the secondary side of the charger can be installed inside the battery pack.

The desk-top unit operates in an open-loop condition and all the functions required to monitor and control the battery charging current are implemented inside the secondary side of the charger. Accordingly, the desk-top unit and the secondary side of the charger are fully isolated in their functions, thereby, eliminating the need for an additional information exchange [6] between them. The operational conditions and circuit parameters of the prototype charger are summarized in Table I. As listed in Table I, the output voltage of the high-frequency rectifier should remain within an 8~20V range to ensure a reliable operation of LT1571-5 used in the charging circuit.

TABLE II: PHYSICAL AND ELECTRICAL PARAMETERS OF PCB WINDINGS

Physical parameters of PCB windings			
Primary winding		Thickness of copper trace	$90 \mu\text{m}$
		Turns of traces	14
		Separation between traces	0.43 mm
		Width of trace	0.82 mm
Secondary winding	Same as the primary winding		
Electrical parameters of PCB windings with 2.4 mm separation			
$L_k = 1.46 \mu\text{H}$, $L_m = 1.02 \mu\text{H}$, $a = 1.57$			
$R_p = R_s = 0.28 \Omega$			

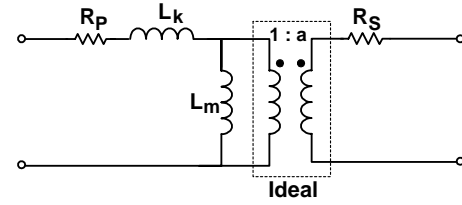


Fig. 3. Circuit model for neighboring PCB windings.

2.2 PCB windings and Circuit Model

Table II shows the physical and electrical parameters of the PCB windings used in the prototype contactless charger. The PCB windings are fabricated on a single-sided PCB with 1mm laminate thickness and $3 \text{ ounce} / \text{ft}^2$ copper layer. The dimensions and geometry of copper traces are empirically determined considering the operating conditions of the charger and circuit properties of the PCB windings. The power handling capacity of the PCB windings is proportional to the area of the copper traces [2], therefore, the size of the PCB windings should be designed according to the power requirement of the application system. In the current design, however, the PCB windings are oversized in an attempt to ensure a continuous operation of the battery charger even with a considerable misalignment between the PCB windings. The 35 mm-diameter spiral PCB windings used in the prototype charger were in fact tested to deliver a 24 W output power at a 68 % efficiency with the copper traces 2.4 mm apart. The geometry of the copper traces directly affects the circuit properties of the PCB windings. Many turns of a thin copper trace enhances the inductance, however, this design also increases winding resistances. The turns and width of the copper traces were designed based on the experimental trade-off study on the performance of the prototype charger. The effects on the dimension and patterns of copper traces on the device properties of the coupled PCB windings have been treated in the recent publication [7].

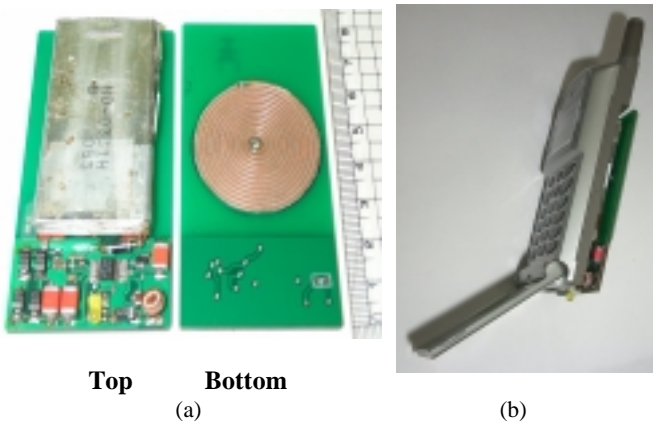


Fig. 4. Secondary side of prototype contactless charger developed for cellular phones. (a) Secondary side of charger. (b) Cellular phone equipped with secondary side of charger.

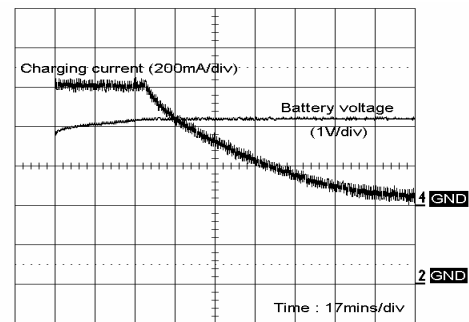
Fig. 3 show a circuit model for the neighboring PCB windings. The circuit model is developed using the conventional method [8] that has been used to model the magnetically coupled inductors. In Fig. 3, the inductive parameter L_k is referred to as the leakage inductance and L_m is called the magnetizing inductance, following the terminologies that have been used to quantify the nonideal characteristics of conventional transformers. The circuit parameters shown in Fig. 3 can be either analytically calculated [9] or experimentally measured [2]. The model parameters measured from the PCB windings separated each other by 2.4 mm (the laminate thickness of two PCBs plus 0.4 mm distance between PCBs) are listed in Table II. Interestingly, the leakage inductance, $L_k = 1.46 \mu H$, is larger than the magnetizing inductance, $L_m = 1.02 \mu H$. These unique characteristics are attributed to the existence of a separation and absence of a magnetic core between the PCB windings. The winding resistances, $R_p = R_s = 0.28 \Omega$, are also important circuit parameters as the ohmic loss in the PCB windings can be a major source of the power losses.

2.3 Performance of Prototype Charger

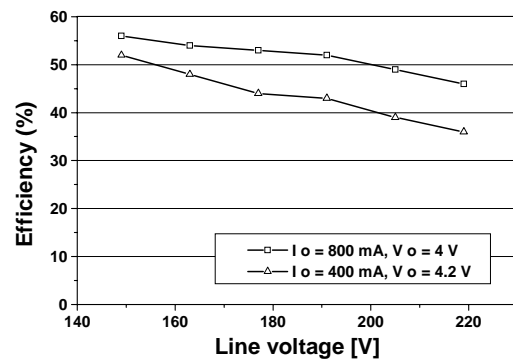
Fig. 4(a) shows the secondary side of the prototype charger fabricated on a double-sided PCB. A 3.3 W lithium-ion battery along with the battery charging circuit is placed on the front side and the secondary PCB winding is printed on the opposite side. Fig. 4(b) shows a cellular phone equipped with the secondary side of the prototype charger. As shown in Fig. 4(b), the secondary side of the charger is naturally suited for a low-profile design and therefore can readily be encapsulated within a standard battery pack



(a)



(b)



(c)

Fig. 5. Prototype charger and its performance. (a) Prototype charger in operation. (b) Charging profile. (c) Efficiency.

without causing major heat management problems. Fig. 5(a) shows the proposed contactless charging system in operation. The prototype charger was found not to adversely affect the performance of the cellular phone. No perceptible consequences of EMI were observed during field tests, however, a newly proposed shielding technique [10] using the ferrite polymer composite sheet can be adapted to the PCB windings to suppress the leakage flux to a negligible level. Fig. 5(b) shows the charging characteristics of the prototype charger that goes through a transition from a constant-current charging to a constant-voltage charging.

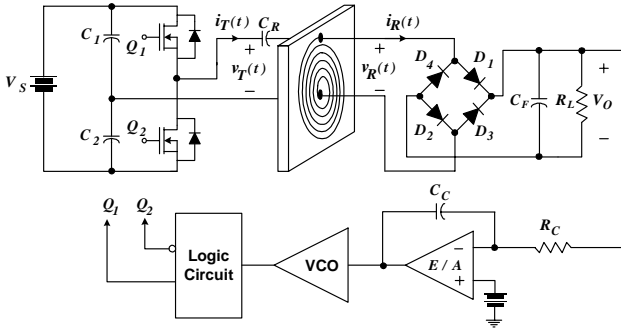


Fig. 6. Simplified circuit diagram of proposed contactless charger.

TABLE III: OPERATIONAL CONDITIONS AND CIRCUIT PARAMETERS OF PROTOTYPE CONVERTER.

Operational Conditions	
$V_S = 40 \sim 60V$, $V_O = 24V$, $R_L = 10\Omega \sim 15\Omega$ ($I_o = 1.6 \sim 2.4A$), $f_s = 670 \text{ kHz} \sim 1.66 \text{ MHz}$	
Circuit Parameters	
Power Stage	Feedback Controller
Q_1 Q_2 : FDD5690 ($r_{DS} = 0.027\Omega$)	Control IC: UC3861DW
C_1 C_2 : $5 \mu\text{F}$ (MLCC)	R_C : $200 \text{ k}\Omega$
C_R : 40 nF (Film)	C_C : 680 pF
$D_1 \sim D_4$: B330A (Schottky)	
C_F : $30 \mu\text{F}$ (MLCC)	

The charger exhibited a precisely controlled charging profile. Fig. 5(c) shows the efficiency of the proposed charger measured with two different conditions: one at constant-current charging (upper curve in Fig. 5(c)) and the other at constant-voltage charging (lower curve in Fig. 5(c)). The maximum efficiency of 57% was measured during a constant-current charging mode. In these measurements, a dc voltage source was used as a substitute for the rectified line voltage.

3. ULTRA LOW-PROFILE DC-TO-DC CONVERTER

3.1 Structure and Circuit Topology

Fig. 6 shows a conceptual schematic diagram of an ultra low-profile dc-to-dc converter that utilizes a pair of PCB windings, etched on the opposite sides of a double-sided PCB, as a coreless transformer. The power stage adapts a half-bridge series resonant circuit that utilizes a PCB transformer as an element of the resonant tank as well as an energy transfer device. The feedback controller employs a frequency modulation control to regulate the output voltage. The operational conditions and circuit parameters of the prototype converter are shown in Table III. The experimental PCB transformer is fabricated on a double-sided PCB with 0.8 mm laminate thickness and 3

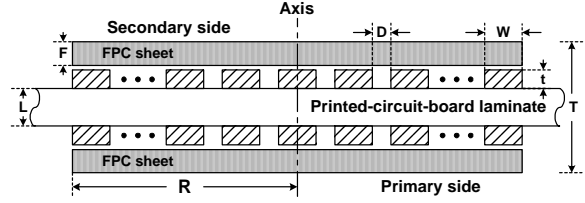


Fig. 7. Simplified circuit diagram of proposed contactless charger.

TABLE IV: DIMENSIONS OF PCB TRANSFORMER

Symbol	Description	Value
T	Thickness of PCB transformer	1.61 mm
R	Radius of PCB transformer	18 mm
	Turns of copper traces	14 Turns
t	Thickness of copper trace	105 μm (3ounce)
D	Distance between copper traces	0.29 mm
W	Width of copper trace	0.97 mm
L	Thickness of PCB laminate	0.8 mm
F	Thickness of FPC sheet	0.3 mm

ounce/ft² copper layer. Two concentric 36 mm-diameter spirals, each printed on the opposite side of a double-sided PCB, are used as the transformer windings. The C351 FPC sheets from EPCOS [11] are attached on the opposite surfaces of the PCB transformer to enclose the magnetic flux. The cross-sectional view of the PCB transformer is depicted in Fig. 7, and the physical dimensions of the PCB transformer are listed in Table IV. The design of the experimental PCB transformer closely follows that of the previous publication [10], however, the application circuit, analysis method, and design approach are different from those of the previous works.

3.2 Performance of Prototype Converter

Fig. 8 shows the two different versions of the prototype low-profile dc-to-dc converter. The upper figure is the appearance of the prototype converter before attaching the FPC sheets on the PCB transformer, while the lower is the final form of the prototype converter with the FPC sheets on the PCB transformer. The converter was fabricated in a 40 mm \times 80 mm area with a 4 mm thickness using surface mount devices for the power stage, control circuit, and other auxiliary circuits. The shielding effect of the self-adhesive C351 FPC sheets is presently limited by its low permeability ($\mu_r = 10.8$), and further improvements are needed to reduce the EMI to a negligible level.

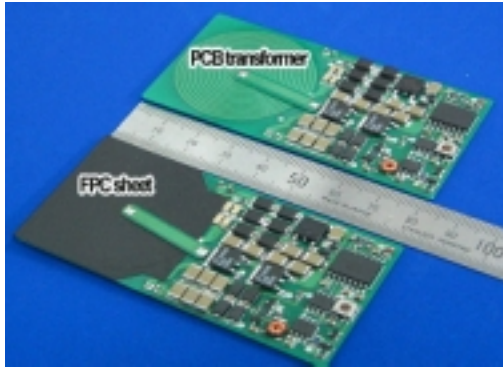


Fig. 8. Prototype low-profile converter with and without FPC sheets on PCB transformer.

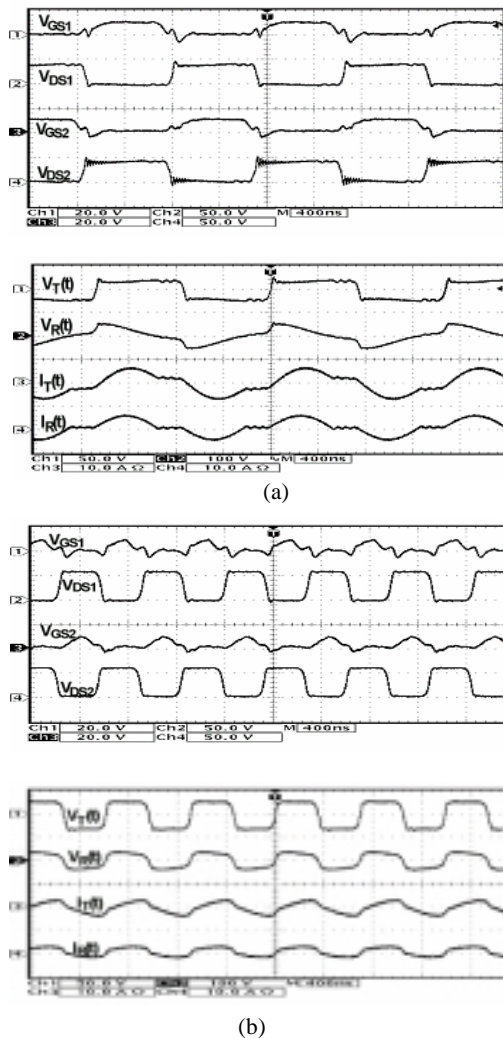


Fig. 9. Experimental waveforms of prototype converter. (a) At operating point of $V_S = 40 V$ and $R_L = 10 \Omega$. (b) At operating point of $V_S = 60 V$ and $R_L = 15 \Omega$.

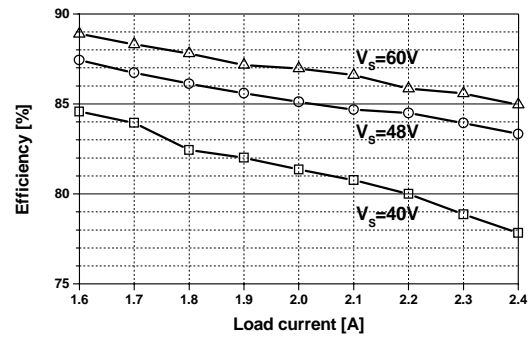


Fig. 10. Efficiency of prototype converter.

Fig. 9 shows the major circuit waveforms of the prototype converter at two different operating points. Fig. 9(a) shows the gate drive signal and drain-source voltage of two MOSFET switches (upper traces) and the circuit waveforms associated with the PCB transformer (lower traces) at the operating point of $V_S = 40 V$ and $R_L = 10 \Omega$. The definitions for the circuit waveforms shown in the lower traces are given in Fig. 6. Fig. 9(b) illustrates the circuit waveforms at the operating point of $V_S = 60 V$ and $R_L = 15 \Omega$. The experimental waveforms demonstrate all the prominent features of the prototype converter including the ZVS operation and frequency modulation control. Fig. 9 also indicates that the operation of the prototype converter is virtually identical to that of a conventional LLC resonant converter [12].

Fig. 10 shows the measured efficiency of the prototype converter. The efficiency increases when the input voltage is increased or the load current is reduced, yielding the maximum efficiency of $\eta = 89\%$ at the operating point of $V_S = 60 V$ and $R_L = 15 \Omega$. The tendency of the efficiency curves confirms that the ohmic losses at the PCB windings are the major portion of the total power loss.

4. SUMMARY

This paper presented ultra low-profile power conditioning circuits developed for the use in future SDR application systems. The proposed power conditioning circuits employ the PCB windings as their energy transfer devices, thereby readily realizing a low-profile design making them applicable to SDR application systems.

This paper presented the structure, circuit topology, and performance of two different power conditioning circuits. The first circuit is a contactless battery charger that employs a pair of neighboring PCB windings as a contactless energy transfer device. A prototype contactless battery charger, developed for application with hand-held electronics, is used as an example to address the design

considerations for the PCB windings and selection of the circuit topology. The paper also demonstrated the performance of the contactless charger adapted to a practical application system. The second circuit is an ultra low-profile dc-to-dc converter that utilizes the PCB windings, etched on the opposite sides of a double-sided PCB, as a substitute for the conventional magnetic core-based transformer. A prototype series resonant converter, fabricated in a 40 mm×80 mm area with a 4 mm thickness while achieving the maximum efficiency of 85 % at a 58 W output power, was used as an example to address the theoretical and practical issues involved in the design and implementation of a PCB transformer-based low profile dc-to-dc converter.

REFERENCES

- [1] S. Y. R. Hui, S. C. Tang, and H. Chung, "Coreless printed-circuit board transformers for signal and energy transfer," *IEE Electron. Lett.*, vol. 34, no. 11, pp. 1052-1054, 1998.
- [2] S. Y. R. Hui, S. C. Tang, and H. Chung, "Optimal operation of coreless PCB transformer-isolated gate drive circuit with wide switching frequency range," *IEEE Trans. Power Electron.*, vol. 14, no. 3, pp. 506-514, May 1999.
- [3] B. Choi, and J. Nho, "Contactless energy transfer using planer printed circuit board windings," *IEE Electron. Lett.*, vol. 37, no.16, pp.1007-1009, 2001.
- [4] S. C. Tang, S. Y. R. Hui and H. Chung, "A low-profile power converter using printed-circuit board (PCB) power transformer with ferrite polymer composite," *IEEE Trans. Power Electron.*, vol. 16, no. 4, pp. 493-498, July 2001.
- [5] LT1572 Data Sheet, Linear Technology Co., Milpitas, CA, 2000.
- [6] C. Kim, D. Seo, J. You, J. Park and B. H. Cho, "Design of a contactless charger for cellular phone," *IEEE Trans. Ind. Electron.*, vol. 48, no. 6, pp. 1238-1247, Dec. 2001.
- [7] C. Fernandez, O. Garcia, R. Prieto, J.A. Cobos, S. Gabriels, and G. Van Der Borgh, " Design issues of a coreless transformer for a contactless application," in *Proc. APEC02*, 2002, pp. 339-345.
- [8] J. W. Nilsson, and S. A. Riedel, "*Electronic circuits*," Prentice Hall, New Jersey, 2001, 6th Ed. Appendix C, pp. 993-1001.
- [9] W. G. Hurley, and M. C. Duffy, "Calculation of self and mutual inductances in planar magnetic structures," *IEEE Trans. on Magn.*, vol. 31, no. 4, pp. 2416-2422, July 1995.
- [10] S. C. Tang, S. Y. R. Hui, and H. Chung, "A low-profile power converter using printed circuit board (PCB) power transformer with ferrite polymer composite," *IEEE Trans. Power Electron.*, vol. 16, no. 4, pp. 493-498, July 2001
- [11] "Ferrite Polymer Composite (FPC) film," EPCOS Product Information, Jan. 2001, <http://www.epcos.de/inf/80/ap/e0001000.htm>.
- [12] M. K. Kazimierczuk, and T. Nandakumar, "Class D voltage switching inverter with tapped resonant inductor," *IEE proceedings-B*, vol. 140, no. 3, pp. 177-185, May 1993

Printed Circuit Board Windings-Based Ultra Low-Profile Power Conditioning Circuits for SDR Application Systems

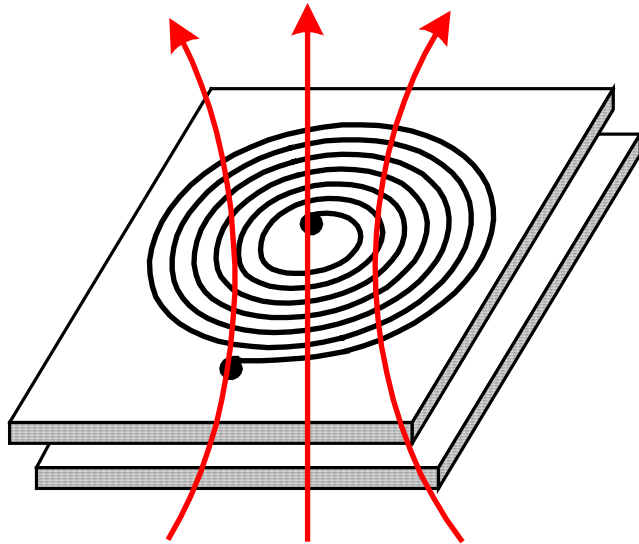
Wonseok Lim, Dongsoo Kim, and Byungcho Choi

**School of Electrical Engineering and Computer Science
Kyungpook National University**

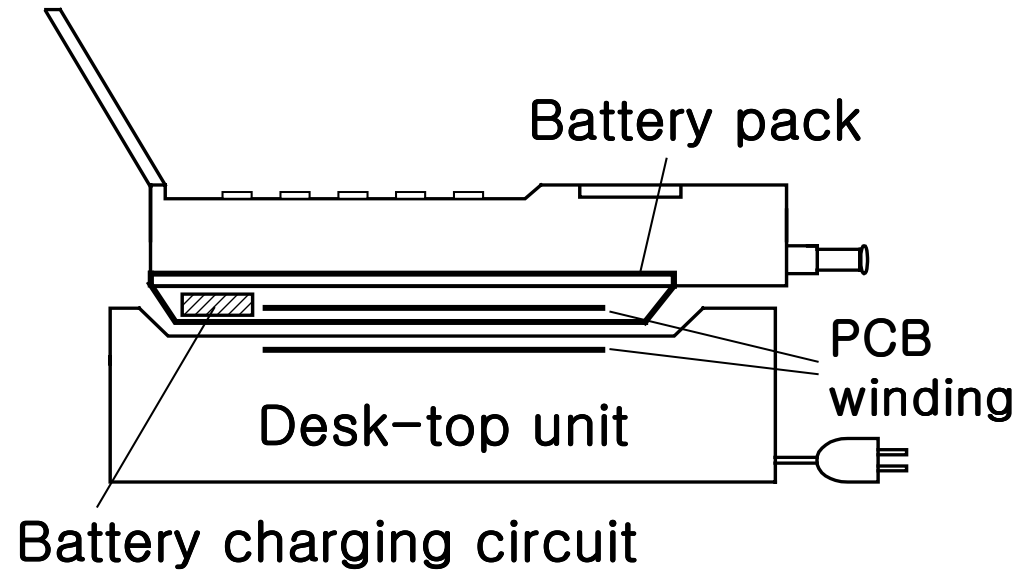
Contactless Battery Charger



Conceptual Diagram

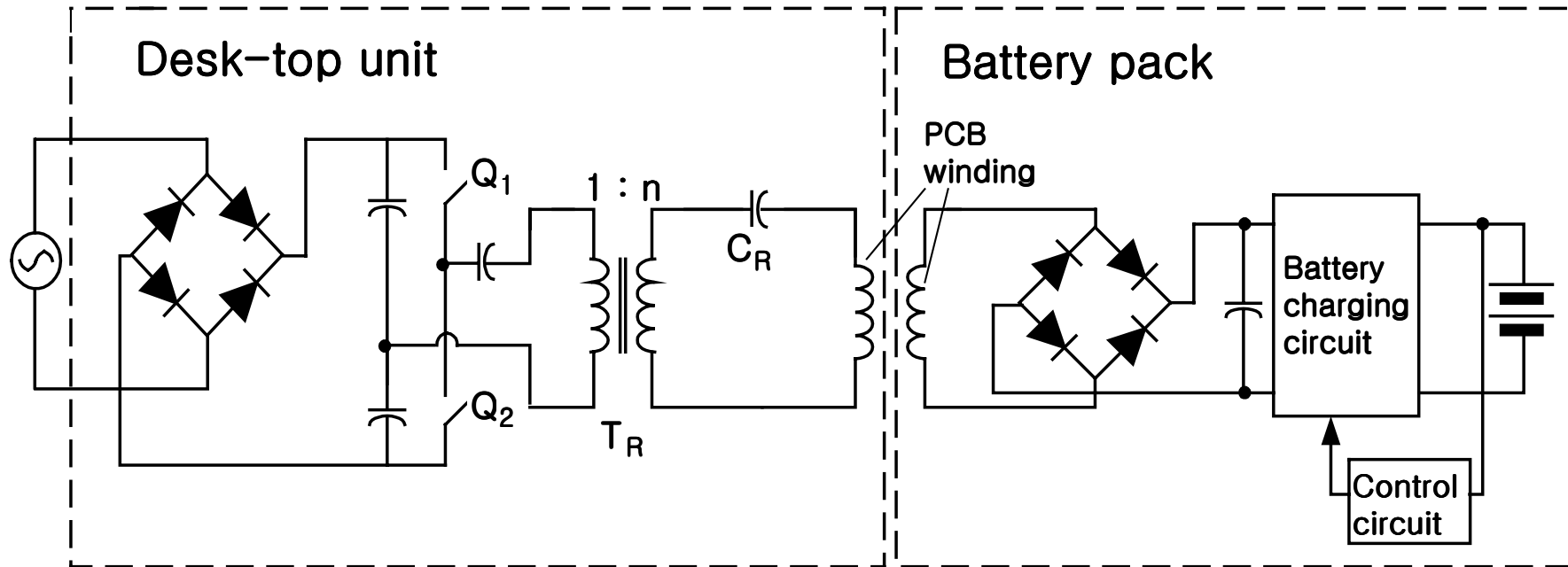


Neighboring PCB windings



Contactless charger

Circuit Diagram

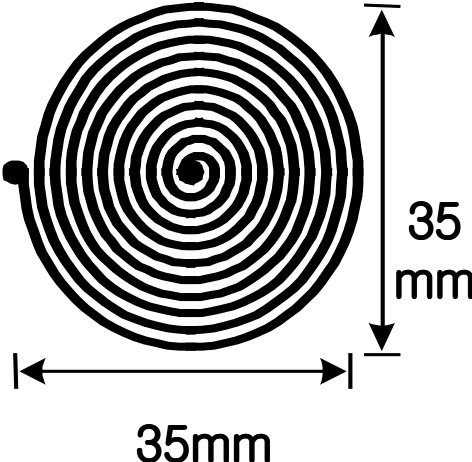


Operational Conditions and Circuit Parameters

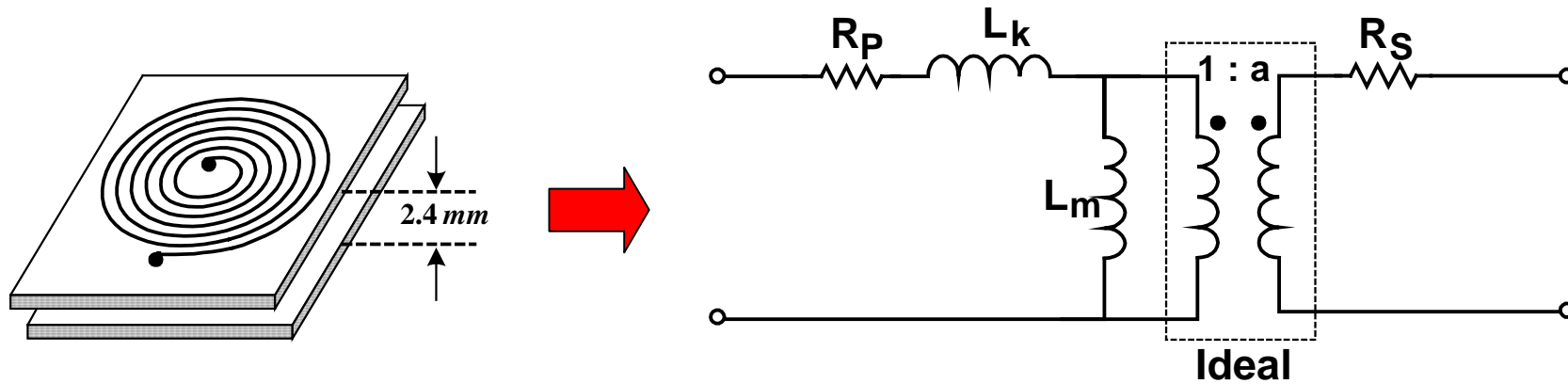
Desk-top unit	Secondary side
Input voltage: $85 \sim 270 V_{ac}$ Switching frequency: $f_S = 950 \text{ kHz}$	Input voltage of battery charging circuit: $8 \sim 20 V_{dc}$ Input current of battery charging circuit: $0.1 \sim 0.35 A_{dc}$
Circuit components: $Q_1 \sim Q_2$: IRF840 C_R : 40 nF $n = 0.1$	Control IC: LT1571-5 Battery: Type: 3.3W Li-ion Dimension: $55\text{mm} \times 31\text{mm} \times 5.5\text{mm}$ Voltage: $3.6 \sim 4.2 V$ Charging current: $0.8 A$ @ fast charging



PCB Windings

Physical parameters of PCB windings			
Primary winding		Thickness of copper trace	$90 \mu m$
		Turns of traces	14
		Separation between traces	$0.43 mm$
		Width of trace	$0.82 mm$
Secondary winding	Same as the primary winding		

Circuit Model and Electrical Parameters

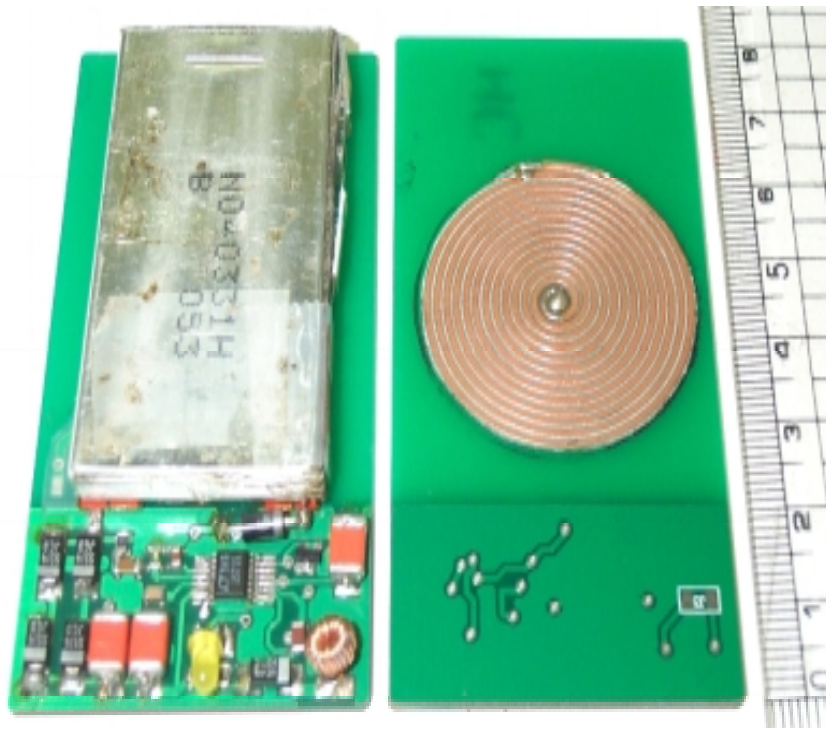


Electrical parameters of PCB windings with 2.4 mm separation

$$L_k = 1.46 \mu H, L_m = 1.02 \mu H, a = 1.57$$

$$R_p = R_s = 0.28 \Omega$$

Secondary Side of Prototype Charger



Top

Bottom

Secondary side of charger

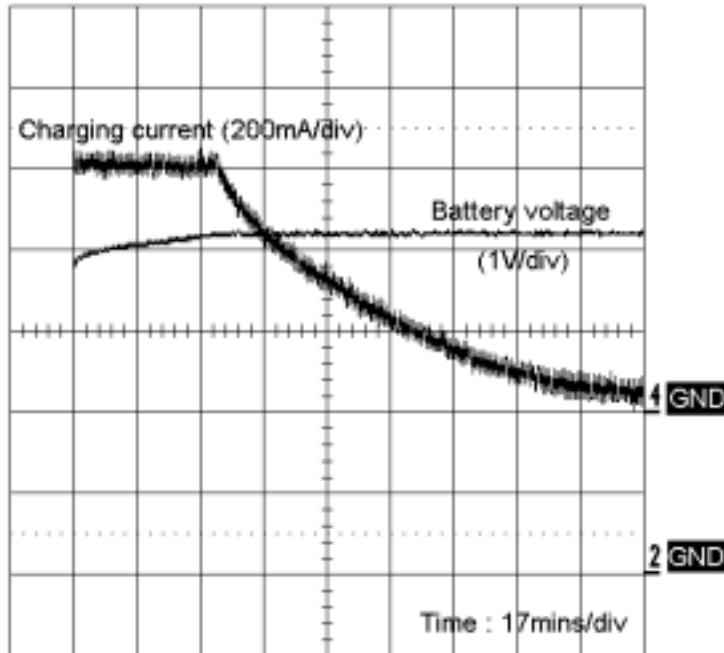


Cellular phone

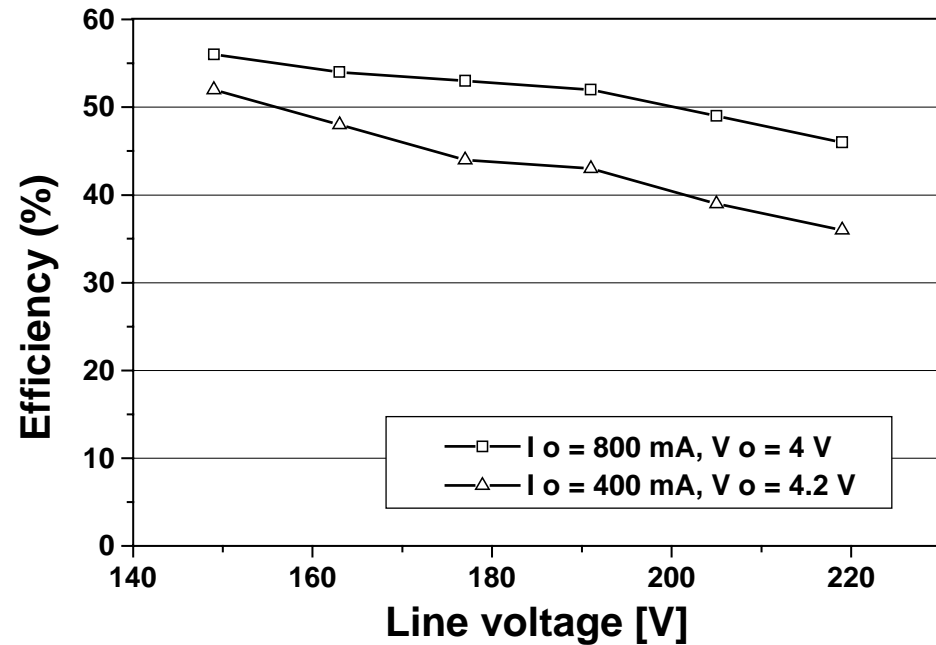
Prototype Charger in Operation



Performance of Prototype Contactless Charger



Charging profile

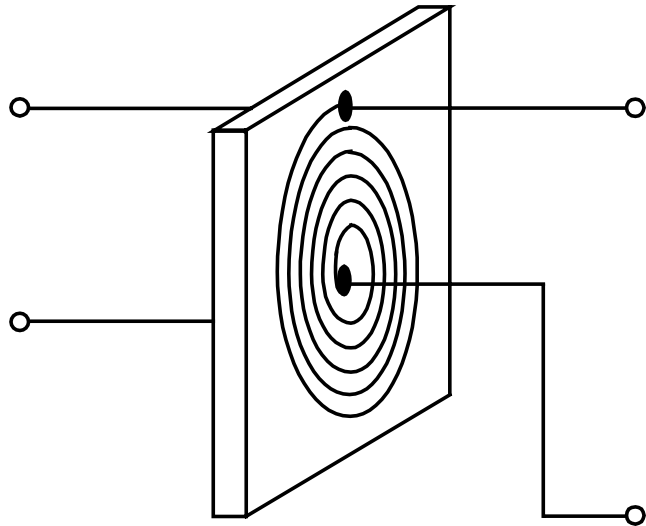


Efficiency

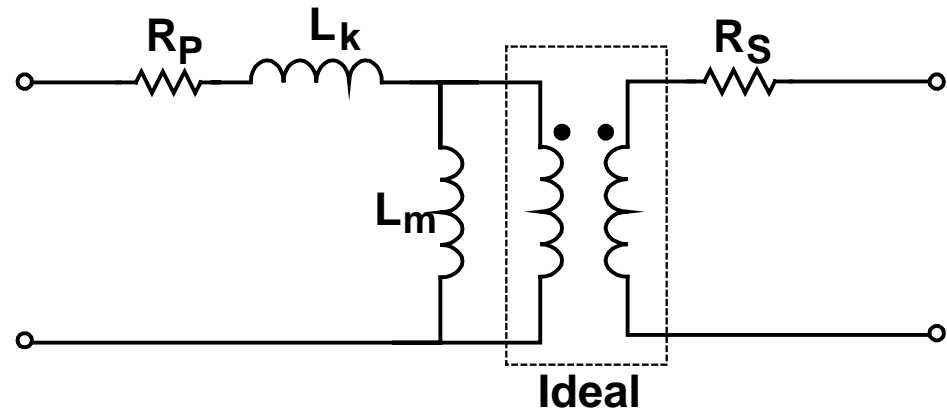
PCB Transformer-Based Low-Profile DC-to-DC Converter



PCB Transformer

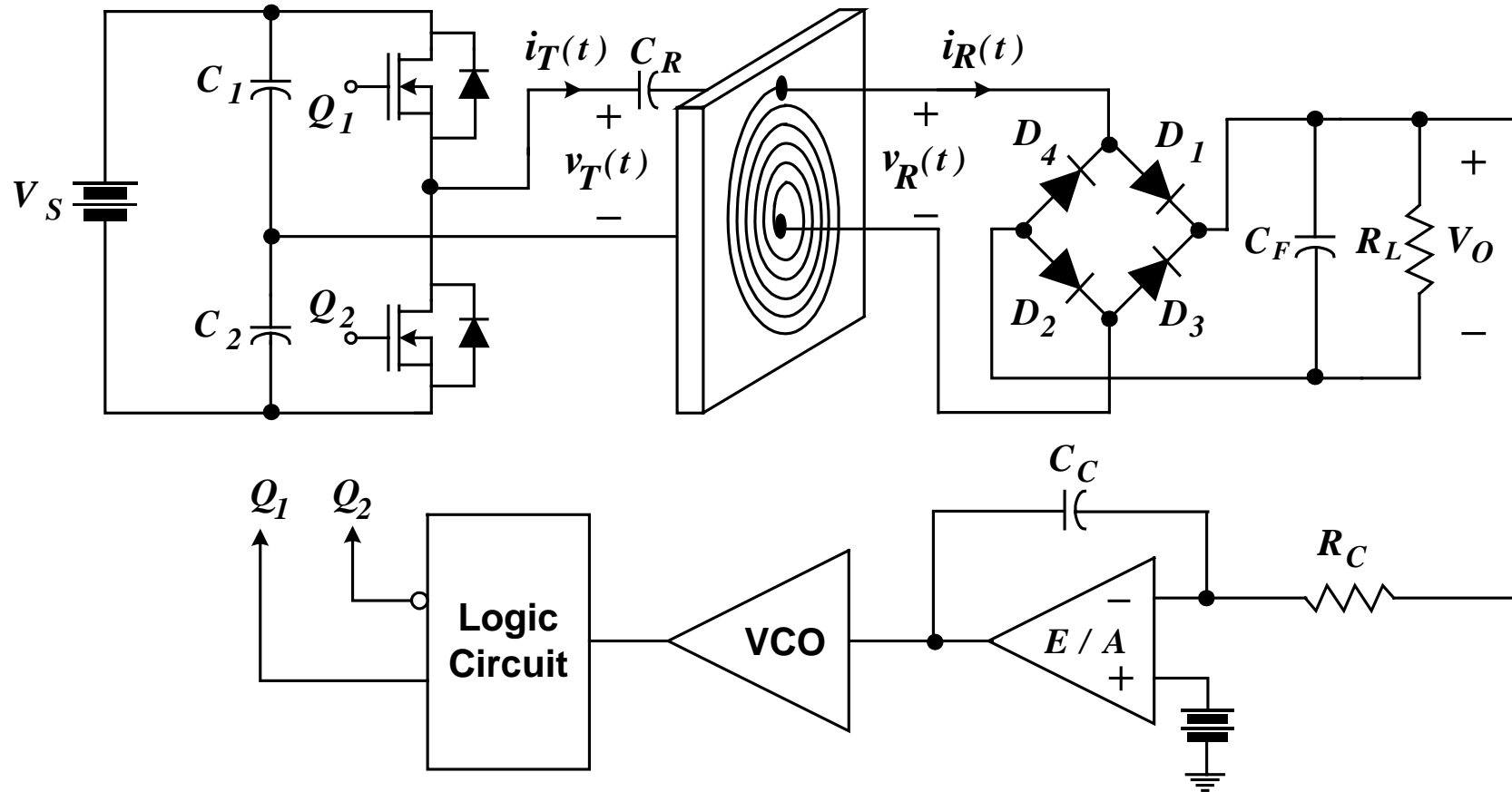


PCB Transformer



Equivalent Circuit Model

Circuit Diagram

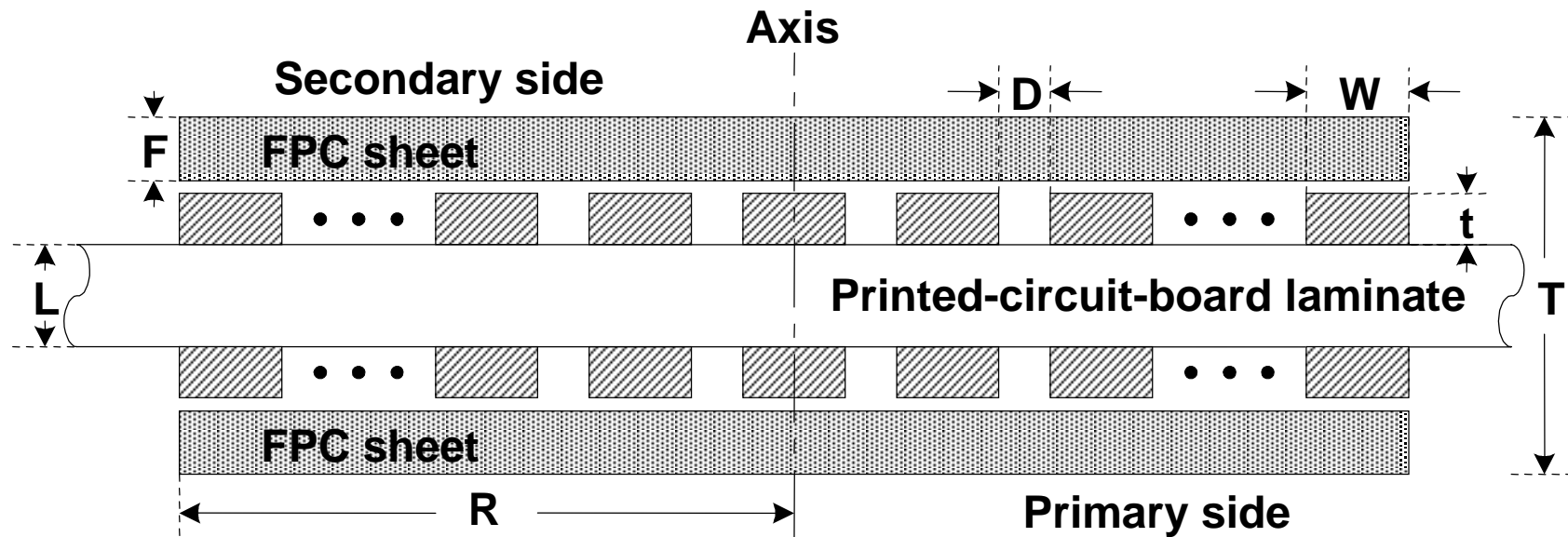


Operational Conditions and Circuit Parameters

Operational Conditions	
$V_S = 40 \sim 60V$, $V_O = 24V$, $R_L = 10\Omega \sim 15\Omega$ ($I_o = 1.6 \sim 2.4A$) , $f_s = 670\text{ kHz} \sim 1.66\text{ MHz}$	
Circuit Parameters	
Power Stage	Feedback Controller
$Q_1 \quad Q_2 : FDD5690$ ($r_{DS} = 0.027\Omega$) $C_1 \quad C_2 : 5\mu F$ (MLCC) $C_R : 40\text{ nF}$ (Film) $D_1 \sim D_4 : B330A$ (Schottky) $C_F : 30\mu F$ (MLCC)	Control IC: UC3861DW $R_C : 200\text{ k}\Omega$ $C_C : 680\text{ pF}$



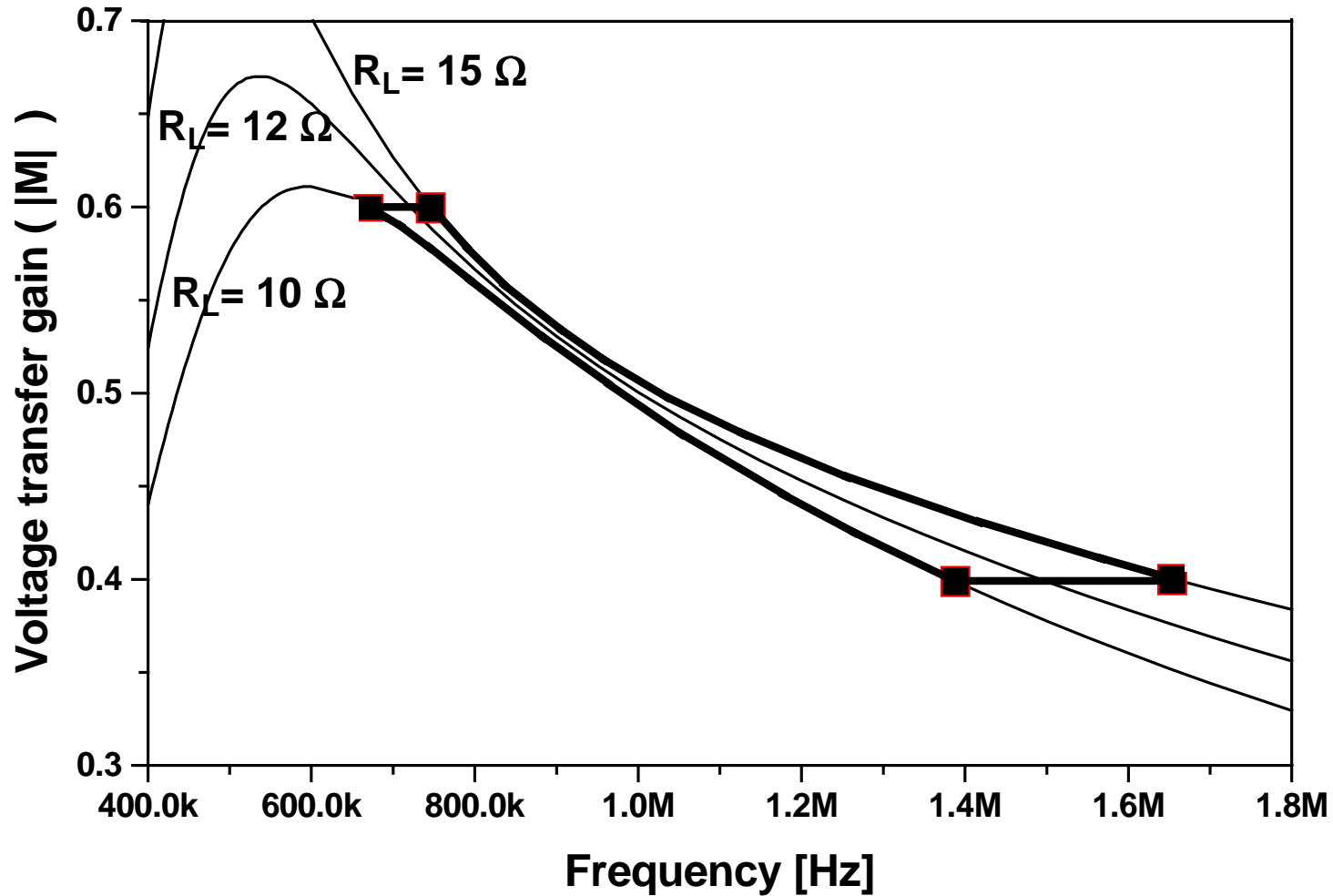
Cross-Section of PCB Transformer



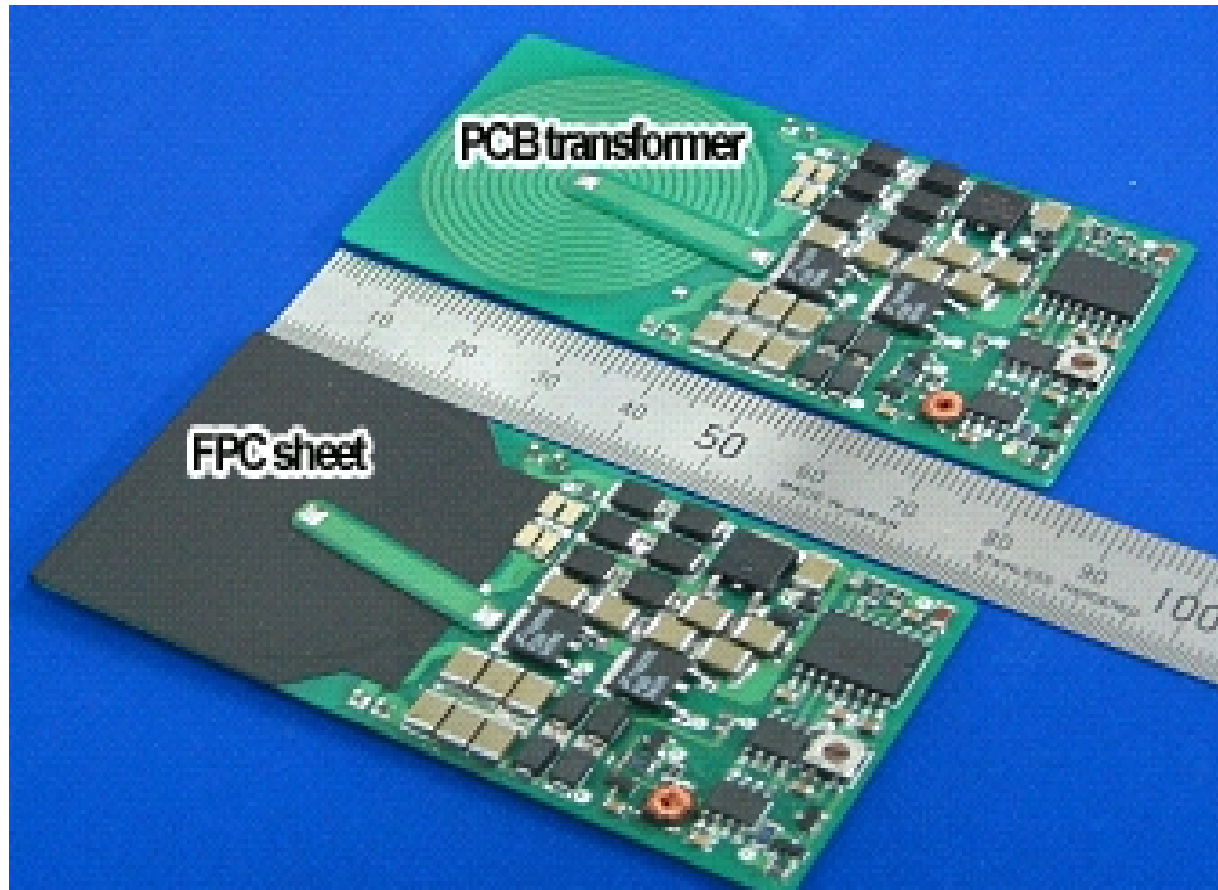
Dimensions of PCB Transformer

Symbol	Description	Value
T	Thickness of PCB transformer	1.61 mm
R	Radius of PCB transformer	18 mm
	Turns of copper traces	14 Turns
t	Thickness of copper trace	$105\mu\text{m}$ (3ounce/ft ²)
D	Distance between copper traces	0.29 mm
W	Width of copper trace	0.97mm
L	Thickness of PCB laminate	0.8 mm
F	Thickness of FPC sheet	0.3mm

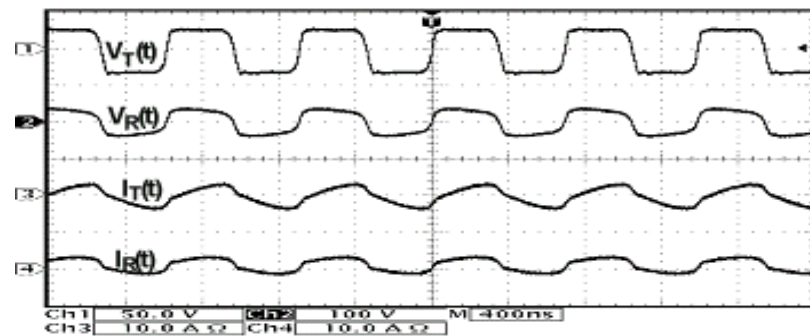
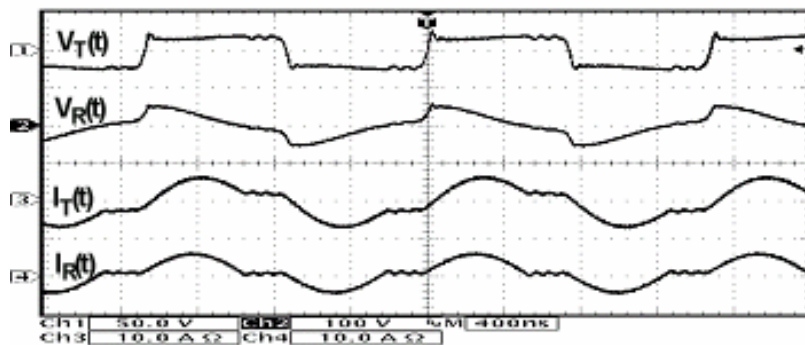
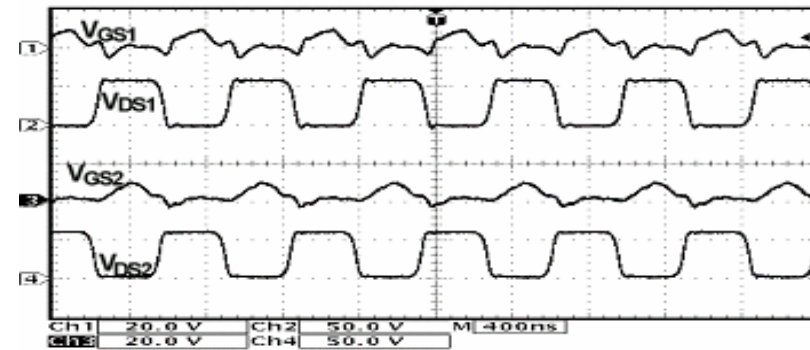
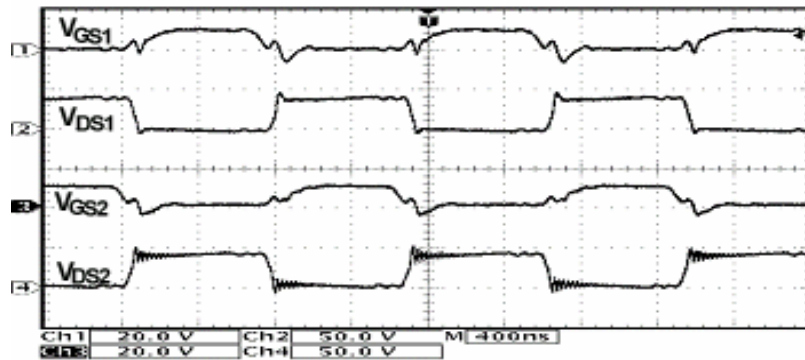
Operational Region



Prototype Converter



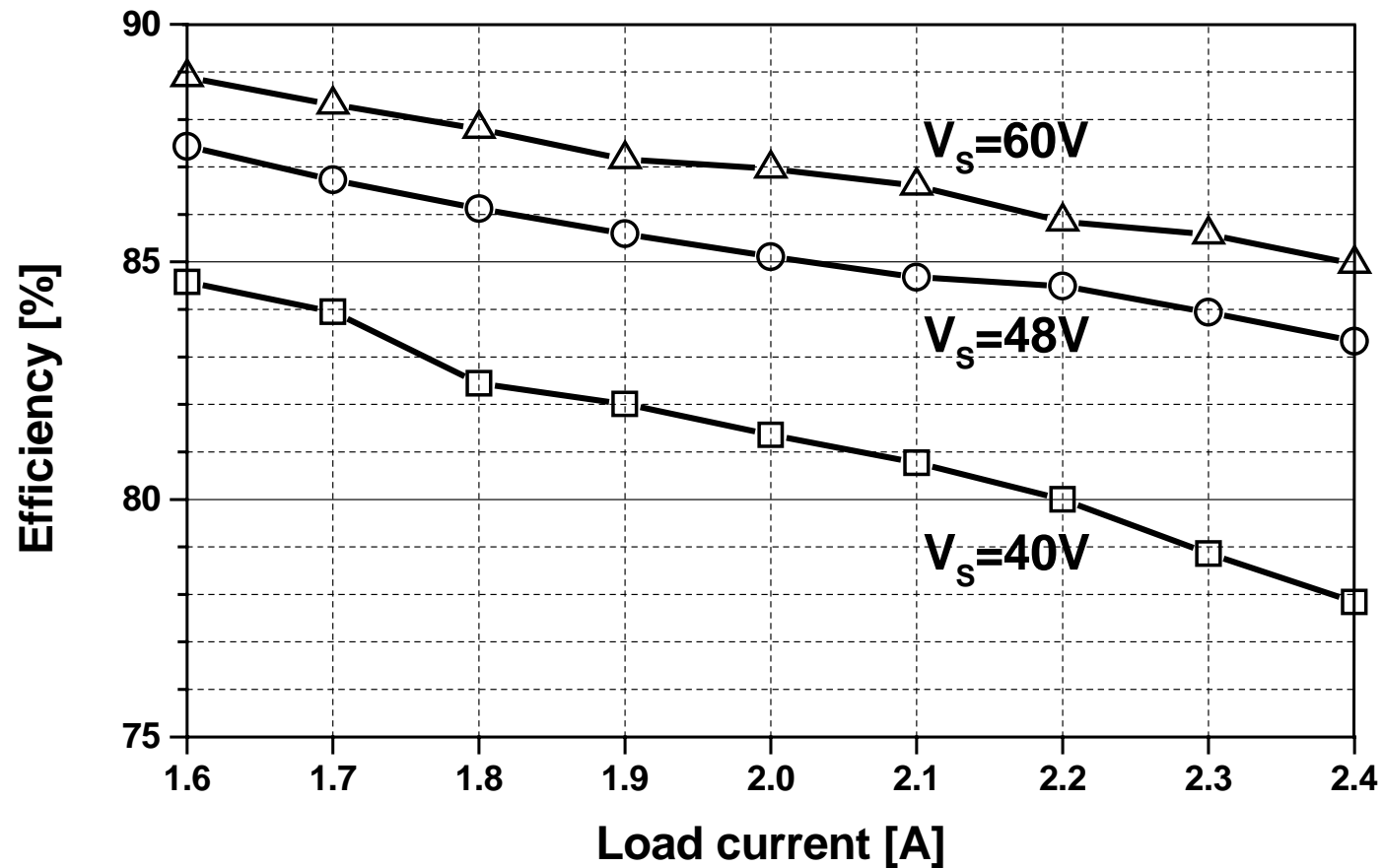
Experimental Waveform of Prototype Converter



$$V_S = 40V \quad R_L = 10\Omega$$

$$V_S = 60V \quad R_L = 15\Omega$$

Efficiency of Prototype Converter



Summary

- **Ultra low-profile power conditioning circuits using PCB windings as energy transfer device**
- **Contactless battery charger for portable hand-held electronics**
- **PCB windings transformer-based low-profile dc-to-dc converter**

